

Enhanced Thrust Due to Ion–Neutral Collisions for Electric Propulsion

Amnon Fruchtman

Received: 5 November 2013/Accepted: 26 January 2014/Published online: 15 February 2014
© Springer Science+Business Media New York 2014

Abstract The enhancement by ion–neutral collisions of the momentum delivered to ions for specified power is compared for acceleration under electric and magnetic pressures. The enhancement in both cases is shown to be proportional to the square-root of the number of collision mean-free-paths when neutral-gas density is low and to the number of collision mean-free-paths when the neutral-gas density is high. The distributions along the acceleration channel of the ion density and velocity and of the electric potential are calculated at the space-charge limit for acceleration by electric pressure and at the diamagnetic-current limit for acceleration by magnetic field pressure, for both collisionless and collisional ions. Optimal magnetic field profile is found for acceleration under magnetic field pressure. Accelerating ions colliding with neutrals under magnetic field pressure can provide a high thrust at a low accelerating voltage.

Keywords Electric propulsion · Thrust over power · Ion-neutral collisions · Ionic wind · Hall thruster

Introduction

A major figure of merit in propulsion in general and in electric propulsion [1] in particular is the thrust per unit of deposited power, the ratio of thrust over power. We have recently demonstrated experimentally and theoretically [2–4], that for a fixed deposited power, the momentum delivered by the electric force is larger if the accelerated ions collide with neutrals during the acceleration. Obviously, the power deposited in the ion current depends only on the potential drop they cross. The momentum imparted, however, depends also on the residence time of the ions in the acceleration region. If ions collide with neutrals after they have been accelerated, then the total momentum of ions and neutrals is the same as without collisions. However, if ions collide while they are being accelerated by the electric

A. Fruchtman (✉)
H.I.T. - Holon Institute of Technology, 52 Golomb St., 58102 Holon, Israel
e-mail: fnfrucht@hit.ac.il

field, their residence time in the acceleration region is increased, due to their slowing-down collisions with neutrals, and the total momentum gained by the flow is enhanced. The electric force is being felt by the ions for a longer time, and the impulse they gain is higher. This larger impulse is redistributed also in the neutral-gas mass through the ion–neutral collisions. In a collisional plasma, most of the momentum gained by the ions from either the electric or magnetic pressure is carried by the neutrals.

The main advantage of electric propulsion is the reduction of the propellant mass needed for a given space mission due to the higher exhaust velocities, relative to those achieved by chemical propulsion. When ions collide with neutrals during the acceleration, however, the average jet velocity is lowered. Therefore, the higher thrust for given power is achieved for a collisional plasma at the expense of a lower thrust per unit mass flow rate, reflecting what is true in general, that the lower the flow velocity (and the so-called specific impulse) is, the higher the thrust for a given power. This is the usual trade-off between having a large specific impulse and a large thrust. Broadening the range of jet velocities and thrust levels is desirable since there are different propulsion requirements for different space missions. Operation in the collisional regime can be advantageous for certain space missions, either for air-breathing propulsion [5, 6], or for short periods of time when the thrust has to be increased and electric power is limited. Indeed, enhancement of the thrust for a given power through ion–neutral collision has been explored in ionic wind propulsion employing high-voltage corona discharges [7–10]. The thrust is provided by the electric pressure and is limited by space charge of the ion flow [11]. In the configuration we were studying, the ions are accelerated in quasi-neutral plasma, where electrons are magnetized, and the thrust is provided by magnetic-field pressure. We note on passing that the momentum over power is also enhanced by ion–neutral collisions in an unmagnetized quasi-neutral plasma where the source of the momentum is not electric or magnetic pressure, but plasma pressure only. This enhancement is also important for propulsion that relies on plasma pressure [12–14].

In this paper we compare the acceleration of collisional plasma by electric and magnetic pressures. The enhancement of thrust delivery by collisions in both cases is shown to be proportional to the square-root of the number of collisions when the neutral-gas density is low and to the number of collisions when the neutral-gas density is high. The momentum transfer from electromagnetic fields to plasma medium is an important basic process. In addition to the understanding gained of this process, our analysis of the similarities and differences between imparting momentum to plasma through electric field and through magnetic field, should be useful in exploring new thruster configurations, in which the thrust over power is large. While similar analysis has been done for the acceleration by electric pressure [7, 11], the analysis for the acceleration by magnetic field pressure and the comparison between the two accelerations is new.

In the analysis we make several simplifying assumptions. The time-independent calculation is one-dimensional (1D) along the acceleration channel. The ion flux density is uniform with no ionization or recombination. We mention, but we do not account here for, possible (and often unavoidable) sources of inefficiency. The distributions along the acceleration channel of the ion density and velocity and of the electric potential are calculated at the space-charge limit for acceleration by electric pressure and at the diamagnetic-current limit for acceleration by magnetic field pressure, for both collisionless and collisional ions. Optimal magnetic field distribution is found for acceleration under magnetic field pressure. The possibility of acceleration of a quasi-neutral collisional plasma by magnetic pressure is attractive since a high thrust density can be achieved with a low accelerating voltage.

In “[The Model](#)” section we present the model. In “[Acceleration by Electric Pressure](#)” section we analyze the collisionless and the collisional ion acceleration under electric pressure. In “[Magnetic Pressure](#)” section we analyze the collisionless and the collisional ion acceleration under magnetic pressure.

The Model

Let us consider neutral gas and ions that are contained in a long and straight tube where the walls are parallel to the x axis. Energy and momentum exchange with lateral walls are neglected. Ions are introduced at one end of the tube, at $x = 0$, and are exiting at the other end at $x = L$. We neglect ionization and recombination, so that Γ , the ion particle flux density along x , is constant. Neutrals that leave the tube at $x = L$ are assumed to be replaced by new neutrals, and the rest of the neutrals are assumed immobile. Therefore, the neutral-gas density N is assumed uniform along the acceleration channel. Employing these simplifying assumptions, we restrict ourselves to an optimal operation with no particle (either ion or neutral) losses.

The configuration we analyze corresponds to a thruster that operates in a steady state, so that our model is time-independent. In addition, the plasma and the electromagnetic fields vary mostly along the tube, so that we use a 1D model in which the variables depend on x only. The governing equations of our time-independent 1D model are the ion and electron momentum equations for the plasma and Gauss and Ampere laws for the electromagnetic fields. The ion momentum equation is

$$\frac{d}{dx}(m\Gamma v) = neE - mv\Gamma, \quad (1)$$

where E is the electric field in the x direction, m and n are the ion mass and density, and v and Γ are the ion velocity and particle flux density (both in the x direction). Also, e is the elementary charge, and v is the ion-neutral collision frequency. The terms on the right-hand side (RHS) of the equation express the forces exerted on the ions (that are assumed unmagnetized). These forces are the electric force and the drag due to ion–neutral collisions. We focus on the acceleration channel, neglect ionization and recombination, so that

$$\Gamma \equiv nv, \quad (2)$$

is constant (and no continuity equation is needed). The electron momentum equation in the x direction is

$$0 = -en_eE - en_ev_{ey}B, \quad (3)$$

where B is the magnetic field (in the z direction), n_e is the electron density and v_{ey} is the electron drift velocity in the y direction. The electric and the magnetic forces on the electrons in the x direction are approximately equal and the (assumed small) electron inertia and pressure terms are neglected in Eq. (3). We note that in the cylindrical geometry of a Hall thruster, the magnetic field is in the r direction (here z), the electrons drift in the azimuthal direction (here y), and the ions are accelerated along z (here x).

The electromagnetic fields are governed by Gauss law,

$$\epsilon_0 \frac{dE}{dx} = e(n - n_e), \quad (4)$$

and by Ampere's law,

$$\mu_0 e n_e v_{ey} = \frac{\partial B}{\partial x}, \quad (5)$$

where ϵ_0 and μ_0 are the permittivity and permeability of free space.

Employing Eq. (5), we write Eq. (3) as

$$0 = -e n_e E - \frac{1}{\mu_0} \frac{\partial B}{\partial x} B. \quad (6)$$

We omitted the pressure terms from both ion and electron momentum equations. As we mentioned in the Introduction, if there is no applied electric or magnetic field, the pressure (usually of the electrons) is a source of thrust. Then the pressure term should be retained in the equations, and an equation of continuity that describes ionization should be added. In this case of quasi-neutral unmagnetized plasma, ion–neutral collisions result in a larger thrust than in a collisionless plasma [13–16].

The ion–neutral collision term is treated here for two cases. When the neutral-gas density is not too high, the ion flow velocity is larger than the neutral-gas thermal velocity. The ion–neutral collision frequency is then approximated as [15, 17, 18]

$$v = \sigma N v, \quad (7)$$

where σ is the ion–neutral collision cross section. At the opposite limit, the neutral-gas density is so high, that the ion flow velocity is reduced by collisions with neutrals and becomes lower than v_T , the neutral-gas thermal velocity. Then, the ion–neutral collision frequency is approximated as

$$v = \sigma v_T N. \quad (8)$$

We treat the two limits of the collision frequency separately to exhibit the different behaviors, instead of using a unified form of the collision term [15], in which case the analysis is less transparent. Because of the dependence of v on the ion velocity v in Eq. (7), we refer to that case as the nonlinear collisions case, and to the other case of Eq. (8) as the linear collisions case.

In the next section we investigate the acceleration under electric pressure at the space-charge limit (SCL).

Acceleration by Electric Pressure

The net electric force per unit volume on a (singly-ionized) plasma in the x direction is $F = e(n - n_e)E$. Employing Gauss law [Eq. (4)], we write this force as $F = (\epsilon_0/2)dE^2/dx$. Integrating along the acceleration channel, we express the thrust density due to the electric field, the electric force per unit area, as $(\epsilon_0/2)[E^2(x = L) - E^2(x = 0)]$, which is the difference in the electric pressure on the two ends of the acceleration channel. At SCL the electric field is zero at the ion injection plane, $E(x = 0) = 0$. Therefore the thrust density is due to the electric pressure and has the form

$$F_E = \frac{\epsilon_0 E_L^2}{2}, \quad (9)$$

where $E_L \equiv E(x = L)$.

We assume that the electron density is zero,

$$n_e = 0, \quad (10)$$

so that Gauss law, Eq. (4), becomes

$$\epsilon_0 \frac{dE}{dx} = en. \quad (11)$$

The governing equations are thus Eqs. (1), (11) and (2). This is the case that ion–neutral collisions create the ion wind effect [7–10]. We treat three separate case in our 1D model; collisionless ions, nonlinear collisions, and linear collisions. We first present a unified treatment of two of the cases, the collisionless and the linear collisions. We will then treat separately each one of the three cases.

The Collisionless and the Linear Collisions Cases

We assume the linear collisions case, Eq. (8), so that v is constant. We take the derivative of Eq. (1) with respect to x , and using Eq. (2) we write

$$mv \frac{d}{dx} \left(v \frac{dv}{dx} \right) = \frac{e^2}{\epsilon_0} \Gamma - mvv \frac{d}{dx} v. \quad (12)$$

It is natural to write the equation with respect to time t along the ion trajectory, $dt \equiv dx/v$, $[t(x = 0) = 0]$, so that we obtain a linear equation in v :

$$m \frac{d^2v}{dt^2} = \frac{e^2}{\epsilon_0} \Gamma - mv \frac{dv}{dt}. \quad (13)$$

The ions are assumed to enter the channel with zero velocity $v(t = 0) = 0$. We restrict ourselves to the SCL case, $E(x = 0) = 0$, so that also $dv/dt(t = 0) = 0$. With these two boundary conditions,

$$v = \frac{e^2 \Gamma}{\epsilon_0 m v^2} [vt + \exp(-vt) - 1]. \quad (14)$$

Integrating the velocity with respect to t , we express L with the ion transit time τ , as

$$L = \frac{e^2 \Gamma}{\epsilon_0 m v^3} \left[\frac{v^2 \tau^2}{2} + 1 - \exp(-v\tau) - v\tau \right]. \quad (15)$$

From Gauss law, $\epsilon_0 dE/dt = env$, and from the assumption of SCL, we write the electric field along the ion trajectory as

$$E = \frac{e}{\epsilon_0} \Gamma t. \quad (16)$$

The voltage becomes

$$\varphi_0 = - \int_0^\tau dt v E = \frac{e^3 \Gamma^2}{\epsilon_0^2 m v^4} \left[1 - \exp(-v\tau) - \frac{(v\tau)^2}{2} + \frac{(v\tau)^3}{3} - v\tau \exp(-v\tau) \right]. \quad (17)$$

For specified L and φ_0 , Eqs. (15) and (17) determine τ and Γ . Then the electric field at the exit $E_L = (e/\epsilon_0)\Gamma\tau$ is determined, as well as the thrust density F_E , which is

$$F_E = \frac{e^2 \Gamma^2}{2\epsilon_0} \tau^2. \quad (18)$$

We write simple analytic expressions for the collisionless and the linear collisional case.

Collisionless Limit: Electric Pressure

Let us assume that

$$v\tau \ll 1, \quad (19)$$

so that the collisional term can be neglected in the momentum equation. At that limit Eqs. (15) and (17) are reduced to $L = e^2 \Gamma \tau^3 / 6\epsilon_0 m$ and $\varphi_0 = e^3 \Gamma^2 \tau^4 / 8\epsilon_0^2 m$. Therefore,

$$\Gamma = \Gamma_{CL} \equiv \frac{2^{5/2} \epsilon_0 \varphi_0^{3/2}}{9(em)^{1/2} L^2}, \quad (20)$$

the regular Child–Langmuir law. The thrust density is

$$F_E = \Gamma (2em\varphi_0)^{1/2} = \frac{8\epsilon_0 \varphi_0^2}{9L^2} \quad (21)$$

The impulse per ion is

$$\frac{F_E}{\Gamma} = (2em\varphi_0)^{1/2}. \quad (22)$$

The thrust over power is

$$\frac{F_E}{e\Gamma\varphi_0} = \left(\frac{2m}{e\varphi_0} \right)^{1/2} = \frac{2}{v_0}, \quad (23)$$

where

$$v_0 \equiv \left(\frac{2e\varphi_0}{m} \right)^{1/2}. \quad (24)$$

The axial profiles of the ion velocity and density and of the potential at the Child–Langmuir limit are

$$v = v_0 \left(\frac{x}{L} \right)^{2/3} \quad n = \frac{4\epsilon_0 \varphi_0}{9eL^2} \left(\frac{L}{x} \right)^{2/3} \quad \varphi = \varphi_0 \left[1 - \left(\frac{x}{L} \right)^{4/3} \right]. \quad (25)$$

In the next subsection we look at the linear collisions limit.

Linear Collisions: Electric Pressure

Let us look at the limit opposite to the limit of the previous subsection,

$$v\tau \gg 1. \quad (26)$$

At that limit, Eqs. (15) and (17) are reduced to $L = e^2 \Gamma \tau^2 / (2\epsilon_0 m v)$ and $\varphi_0 = e^3 \Gamma^2 \tau^3 / [3\epsilon_0^2 m v]$. The space-charge limited ion flux density is reduced by collisions from the Child–Langmuir value to

$$\Gamma = \frac{9\epsilon_0\varphi_0^2}{8mvL^3} = \frac{81}{32(2)^{1/2}} \left(\frac{v_0/v_T}{\sigma NL} \right) \Gamma_{CL}. \quad (27)$$

Here, we used the expression (8) for v . The ion flux density reduction is proportional to $(v_0/v_T)/\sigma NL$. The thrust density is

$$F_E = \frac{8\epsilon_0}{9} \left(\frac{\varphi_0}{L} \right)^2. \quad (28)$$

The impulse per ion is

$$\frac{F_E}{\Gamma} = mv_T\sigma NL, \quad (29)$$

and the thrust over power is

$$\frac{F_E}{e\Gamma\varphi_0} = \frac{2(\sigma NL)v_T}{v_0^2}, \quad (30)$$

both increase by $\sigma NLv_T/v_0$ relative to the collisionless Child-Langmuir limit. The quantity σNL expresses the number of ion-neutral collision mean-free-paths along the channel. The axial profiles of the ion velocity and density and of the potential in the linear collisions case are

$$v = \frac{3}{4} \frac{v_0^2}{(\sigma NL)v_T} \left(\frac{x}{L} \right)^{1/2} \quad n = \frac{3\epsilon_0\varphi_0}{4eL^2} \left(\frac{L}{x} \right)^{1/2} \quad \varphi = \varphi_0 \left[1 - \left(\frac{x}{L} \right)^{3/2} \right]. \quad (31)$$

In the next subsection we address the nonlinear collisions case. The condition for the nonlinear collisions case to hold is that $v \gg v_T$, or when

$$\sigma NL \ll \frac{v_0^2}{v_T^2}. \quad (32)$$

For $\varphi_0 = 25$ kV, $L = 4$ cm, atmospheric pressure air ($\sigma \approx 10^{-18}$ m²) at 300 K (typical ionic wind parameters [7–10]), σNL and v_0^2/v_T^2 are both about 10^6 . Therefore, operation at each of the two regimes is possible when parameters are varied.

Nonlinear Collisions: Electric Pressure

In the nonlinear collisions case, Eq. (7) holds, and $v = \sigma Nv$, linear in v . When ions are collisional, the drag by ion–neutral collisions balances approximately the electric force [2–4]. We then neglect the ion inertia in Eq. (1) and the resulting approximated equation is

$$0 = eE - m\sigma Nv^2. \quad (33)$$

We also use again Gauss law, Eq. (4), and obtain the ion velocity as $v = (3e^2\Gamma x/2m\sigma N\epsilon_0)^{1/3}$. Note that near the origin our solution is not a good approximation, since the convective term is not negligible there. The velocity near the origin should be the collisionless solution, $v \cong x^{2/3}$, $vdv/dx \cong x^{1/3}$ while the collisional term is $\cong x^{4/3}$ and is smaller.

We now integrate the electric field $E = (em\sigma N)^{1/3}(3\Gamma x/2\epsilon_0)^{2/3}$ along the acceleration region, so that we can express the space-charge limited ion flux density as

$$\Gamma = \frac{2}{3} \left(\frac{5}{3}\right)^{3/2} \frac{\epsilon_0 \varphi^{3/2}}{(em\sigma N)^{1/2} L^{5/2}} = 3 \left(\frac{5}{6}\right)^{3/2} \frac{\Gamma_{CL}}{(\sigma NL)^{1/2}}. \quad (34)$$

The thrust density is

$$F_E = \frac{25\epsilon_0}{18} \left(\frac{\varphi_0}{L}\right)^2. \quad (35)$$

The impulse per ion is

$$\frac{F}{\Gamma} = 0.363 m v_0 (\sigma NL)^{1/2}, \quad (36)$$

and the thrust over power is

$$\frac{F}{e\Gamma\varphi_0} = 0.363 \times \frac{2}{v_0} (\sigma NL)^{1/2}. \quad (37)$$

Here, $0.363 = 3^{3/2} \times 5^{1/2}/32$. The thrust over power is proportional to $(\sigma NL)^{1/2}$, the square root of the number of collision mean-free-paths along the channel.

We now express the various distributions along the acceleration region. The axial profiles of the ion velocity and density and of the potential in the nonlinear collisions case are

$$v = \left(\frac{5}{6}\right)^{1/2} \frac{v_0}{(\sigma NL)^{1/2}} \left(\frac{x}{L}\right)^{1/3}, \quad n = \frac{10}{9} \frac{\epsilon_0 \varphi_0}{e L^2} \left(\frac{L}{x}\right)^{1/3}, \quad \varphi = \varphi_0 \left[1 - \left(\frac{x}{L}\right)^{5/3}\right]. \quad (38)$$

Figure 1 shows the normalized ion velocity and potential for collisionless ions and for the nonlinear collisions case [Eqs. (25) and (38)]. The corresponding curves for the third case of linear collisions lie between the curves of the two cases shown. Note that the dimensional ion velocity is much smaller in the collisions cases. Figure 2 shows the thrust over power versus σNL under electric pressure acceleration. On the left-side of the figure the nonlinear collisions are dominant [Eq. (37)] and on the right-side the linear collisions dominate [Eq. (30)]. In this example $v_0 = 2.18 \times 10^5 \text{ m s}^{-1}$ and $v_T = 397 \text{ m s}^{-1}$, corresponding to $\varphi_0 = 10 \text{ kV}$, gas at 300 K and atomic number 40 (argon). The transition between the two cases is at $\sigma NL = (v_0/v_T)^2 = 3.025 \times 10^5$.

Magnetic Pressure

Having described the enhanced thrust over power under electric pressure, we turn now to examine the enhanced thrust over power under magnetic pressure. The electron mobility across a magnetic field is impeded. As a result, the plasma electrons do not screen the electric field that is applied across a magnetized plasma. In Hall thruster configurations, that employ crossed electric and magnetic fields, the plasma is quasi-neutral [1]. Thus, we here assume that a quasi-neutral plasma

$$n_e = n, \quad (39)$$

is accelerated by magnetic pressure. Because of quasi-neutrality, we do not use Gauss law. The governing equations are Eqs. (1), (6) and (2). The plasma electrons are usually emitted from a cathode near the exit and move up the potential, crossing magnetic field lines. The flow dynamics thus depends on the cross-field transport of the electrons. A too large electron current causes a power loss and is a source of inefficiency. An additional equation is needed

Fig. 1 Acceleration under electric pressure. The normalized ion velocity (solid line) and potential (dashed-dotted) for collisionless ions and the normalized ion velocity (dotted) and potential (dashed) in the nonlinear collisions case

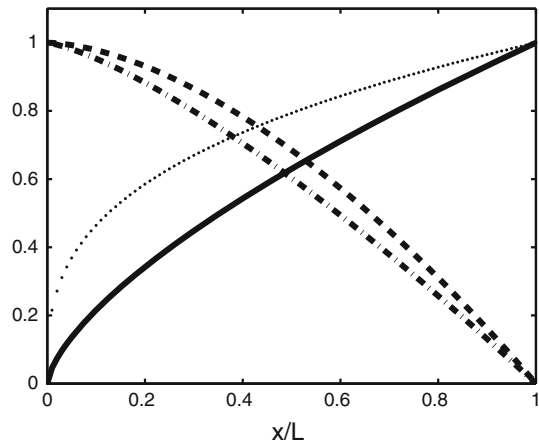
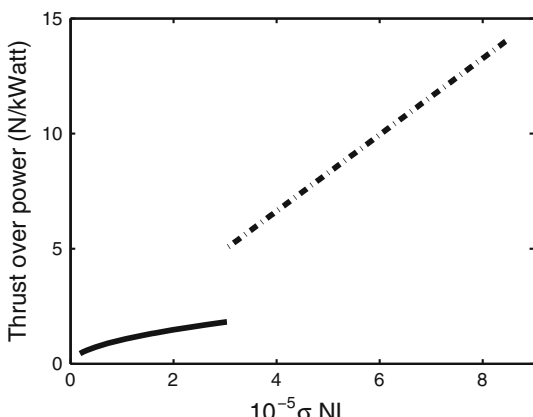


Fig. 2 The thrust over power versus σNL under electric pressure acceleration: $v_0 = 2.18 \times 10^5 \text{ m s}^{-1}$ and $v_T = 397 \text{ m s}^{-1}$, corresponding to $\varphi_0 = 10 \text{ kV}$, gas at 300 K and atomic number 40 (argon). On the left-side of the figure the nonlinear collisions are dominant and on the right-side the linear collisions dominate. The transition between the two regimes is at $\sigma NL = (v_0/v_T)^2$ and $(v_0/v_T)^2 = 3.025 \times 10^5$



to describe the electron cross field transport. However, we focus here on the energy and momentum exchange between the electromagnetic fields and ions and neutrals. We therefore assume that electrons are injected from segmented electrodes along the lateral walls along magnetic field lines, as described in [19], so that no additional equation is needed.

The electrons perform an $\vec{E} \times \vec{B}$ drift in the y direction in our notation. This electron drift results in the Hall current, as it is called in Hall thrusters, the current that generates the $\vec{J} \times \vec{B}$ force on the plasma. Although it has been recently shown that the diamagnetic character of the Hall current affects the performance of thrusters [20], the Hall current in present-day Hall thrusters is too small to modify the applied magnetic field. However, we are interested to explore the case of maximal thrust, which is at what we call the diamagnetic current limit. If the maximal magnetic field is B_0 , the diamagnetic current limit is

$$\mu_0 \int_0^L dx e n v_{ey} = B_0 \implies B(x = L) = 0. \quad (40)$$

When Eq. (40) is satisfied, the flow gains the maximal momentum from the applied magnetic pressure. The thrust density due to magnetic pressure, F_B , is then

$$F_B = \frac{B_0^2}{2\mu_0}. \quad (41)$$

Collisionless Limit: Magnetic Pressure

We neglect the collision term in Eq. (1) so that from energy conservation for the ions we obtain

$$v = \left[\frac{2e(\varphi_0 - \varphi)}{m} \right]^{1/2}. \quad (42)$$

Adding Eqs (1) and (6) we obtain that ions gain all the momentum from the magnetic pressure,

$$m\Gamma v = \frac{B_0^2 - B^2}{2\mu_0}. \quad (43)$$

The last two equations express a relation between the magnetic field, the potential and the ion flux. Using Eq. (40), we obtain that

$$\Gamma = \Gamma_{DM} \equiv \frac{1}{(2me\varphi_0)^{1/2}} \left(\frac{B_0^2}{2\mu_0} \right). \quad (44)$$

Here we denote by Γ_{DM} the collisionless diamagnetic current limit. The potential is written as

$$\varphi = \varphi_0 \left[1 - \left(1 - \frac{B^2}{B_0^2} \right)^2 \right]. \quad (45)$$

The impulse per ion is

$$\frac{F_B}{\Gamma} = (2me\varphi_0)^{1/2}, \quad (46)$$

and the thrust over power is

$$\frac{F_B}{e\Gamma\varphi_0} = \frac{2}{v_0}, \quad (47)$$

as in the collisionless acceleration under electric pressure. The axial profiles of the ion velocity and density with respect to the magnetic field intensity are

$$v = v_0 \left(1 - \frac{B^2}{B_0^2} \right), \quad n = \frac{1}{2e\varphi_0(1 - B^2/B_0^2)} \left(\frac{B_0^2}{2\mu_0} \right). \quad (48)$$

In the next subsection we analyze the case of linear collisions.

Linear Collisions: Magnetic Pressure

We assume that the collision term is high enough so that we neglect the ion inertia term in Eq. (1). Adding Eqs. (1) and (6), we obtain a momentum balance equation; the magnetic force is balanced by the collision force on the ion fluid. We first assume that the neutral-gas density is high enough so that Eq. (8) holds. The momentum balance equation,

$$0 = mv\Gamma + \frac{1}{\mu_0} \frac{\partial B}{\partial x} B, \quad (49)$$

is integrated so that the ion flux density and the magnetic field profile are determined:

$$\Gamma = \frac{B_0^2}{2\mu_0 m v L} = \frac{v_0}{\sigma N L v_T} \Gamma_{DM}, \quad (50)$$

and

$$B = B_0 \left(1 - \frac{x}{L}\right)^{1/2}. \quad (51)$$

The ion flux is reduced by $\sigma N L v_T / v_0$ relative to its value at the collisionless diamagnetic current limit. The potential profile $\varphi(x)$ can be specified arbitrarily along x , for example through segmented electrodes at the lateral wall [19], as mentioned above. The distribution of φ is independent of the magnetic field profile (and of the diamagnetic current profile). The plasma density and velocity are determined through

$$n = B_0^2 / (2\mu_0 L e E), \quad v = e E / m \sigma N v_T. \quad (52)$$

The impulse per ion and the force over power become

$$\frac{F_B}{\Gamma} = m \sigma N L v_T; \quad \frac{F_B}{e \Gamma \varphi_0} = \frac{2 \sigma N L v_T}{v_0^2} \quad (53)$$

which is $(\sigma N L) v_T / v_0$ larger than in the collisionless case.

In the next subsection we examine the case of nonlinear collisions. Assuming a potential of the form $\varphi = \varphi_0(1 - x/L)$ for v in Eq. (52), we obtain that the condition for the linear collisions to hold ($v \leq v_T$) is $2\sigma N L \geq v_0^2 / v_T^2$, which is similar to Eq. (32) in the acceleration under electric pressure.

Nonlinear Collisions: Magnetic Pressure

We use Eq. (7) for the collision frequency, so that Eqs. (1) and (6) are

$$0 = e E - m \sigma N v^2; \quad 0 = \Gamma e E + \frac{v}{\mu_0} \frac{\partial B}{\partial x} B. \quad (54)$$

From these equations we express the electric field as

$$E = \frac{1}{em\sigma N \Gamma^2} \left[\frac{\partial}{\partial x} \left(\frac{B^2}{2\mu_0} \right) \right]^2, \quad (55)$$

and therefore the voltage is

$$\varphi_0 = \frac{1}{em\sigma N L \Gamma^2} \int_0^L G dx, \quad (56)$$

where

$$G \equiv L \left[\frac{\partial}{\partial x} \left(\frac{B^2}{2\mu_0} \right) \right]^2. \quad (57)$$

The ion flux density is then expressed as

$$\Gamma = \left(\frac{\int_0^L G dx}{e\varphi_0 m \sigma N L} \right)^{1/2}. \quad (58)$$

The impulse per ion and the force over power become

$$\frac{F_B}{\Gamma} = \left(\frac{B_0^2}{2\mu_0} \right) \left(\frac{e\varphi_0 m \sigma N L}{\int_0^L G dx} \right)^{1/2}; \quad \frac{F_B}{e\Gamma\varphi_0} = \frac{2}{v_0} \left(\frac{B_0^2}{2\mu_0} \right) \left(\frac{\sigma N L}{\int_0^L G dx} \right)^{1/2}, \quad (59)$$

We look for the magnetic field profile that satisfies the boundary conditions, $B^2(x = 0) = B_0^2$ and $B^2(x = L) = 0$, for which $\int_0^L G dx$ is minimal. We make a simple use of a variation method and solve the corresponding Euler's equation

$$\frac{d}{dx} \left(\frac{\partial G}{\partial (\partial B^2 / \partial x)} \right) - \frac{\partial G}{\partial B^2} = 0. \quad (60)$$

The solution is

$$\frac{\partial B^2}{\partial x} = \text{const}, \quad (61)$$

so that the optimal magnetic field profile, for which the thrust over power is maximal, is

$$B = B_0 \left(1 - \frac{x}{L} \right)^{1/2}, \quad (62)$$

For such a magnetic field profile, $\int_0^L G dx = (B_0^2/2\mu_0)^2$. and therefore the ion flux density is

$$\Gamma = \frac{1}{(m e \varphi_0 \sigma N L)^{1/2}} \left(\frac{B^2}{2\mu_0} \right) = \left(\frac{2}{\sigma N L} \right)^{1/2} \Gamma_{DM}, \quad (63)$$

which is $(2/\sigma N L)^{1/2}$ smaller than the ion flux density at the collisionless diamagnetic current limit. The impulse per ion is

$$\frac{F_B}{\Gamma} = m v_0 \left(\frac{\sigma N L}{2} \right)^{1/2}, \quad (64)$$

and the thrust over power is

$$\frac{F_B}{e\varphi_0 \Gamma} = \frac{2}{v_0} \left(\frac{\sigma N L}{2} \right)^{1/2}, \quad (65)$$

both being larger by $(\sigma N L/2)^{1/2}$ relative to the collisionless case. The potential, ion velocity, and plasma density along the acceleration channel are

$$\varphi = \varphi_0 \left(1 - \frac{x}{L} \right), \quad v = \frac{v_0}{(2\sigma N L)^{1/2}}, \quad n = \frac{\Gamma}{v_0} (2\sigma N L)^{1/2}. \quad (66)$$

Note that the ion velocity and the plasma density are uniform. The condition for the non-linear collisions to be dominant is $2\sigma N L \leq v_0^2/v_T^2$ similar to Eq. (32) (of electric pressure).

Fig. 3 Acceleration under magnetic field pressure. The normalized ion velocity (solid line) and potential (dashed-dotted) for collisionless ions and the normalized ion velocity (dotted) and potential (dashed) in the nonlinear collisions case. The profiles are calculated for the optimal magnetic field profile [Eq. (62)]

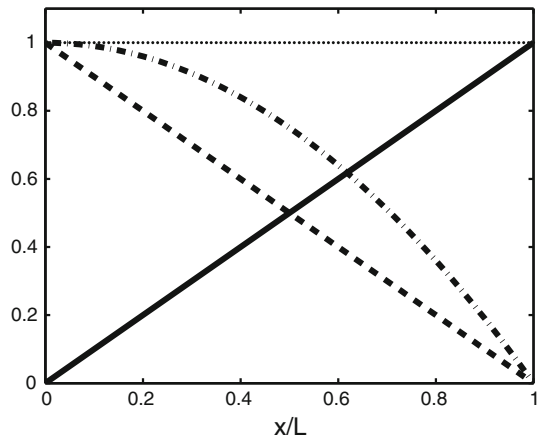


Fig. 4 The thrust over power versus σNL under magnetic pressure acceleration: $v_0 = 3.10 \times 10^4 \text{ m s}^{-1}$ and $v_T = 397 \text{ m s}^{-1}$, corresponding to $\varphi_0 = 200 \text{ V}$, gas at 300 K and atomic number 40 (argon). On the left-side of the figure the nonlinear collisions are dominant and on the right-side the linear collisions dominate. The transition between the two regimes is again at $\sigma NL = (v_0/v_T)^2$ and $(v_0/v_T)^2 = 6084$ in this example

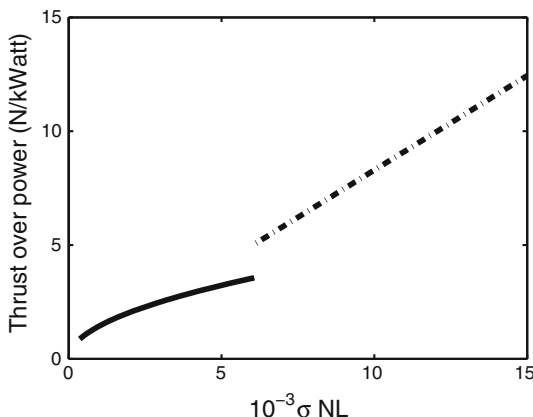


Figure 3 shows the normalized ion velocity and potential for collisionless ions and for the nonlinear collisions case [Eqs. (48) and (66)]. Note that the dimensional ion velocity is much smaller in the collisions cases. The profiles are calculated for the optimal magnetic field profile [Eq. (62)]. Figure 4 shows the thrust over power versus σNL under magnetic pressure acceleration. In this example $v_0 = 3.10 \times 10^4 \text{ m s}^{-1}$ and $v_T = 397 \text{ m s}^{-1}$, corresponding to $\varphi_0 = 200 \text{ V}$, gas at 300 K and atomic number 40 (argon). The thrust over power in the collisionless case [Eq. (47)] is 0.065 N/kW , which is similar to what is achieved by current high-efficiency Hall thrusters. The figure demonstrates that the thrust over power can be increased dramatically by ion-neutral collisions. On the left-side of the figure the nonlinear collisions are dominant [Eq. (65)] and on the right-side the linear collisions dominate [Eq. (53)]. The transition between the two cases is again at $\sigma NL = (v_0/v_T)^2 = 6084$ in this example. In the acceleration by magnetic pressure, the potential used is much lower.

We have shown that in both electric and magnetic pressure accelerations the thrust over power is enhanced by ion-neutral collisions linearly with the square root of the number of mean-free-paths, σNL , when the neutral-gas density is low, and linearly with σNL when the neutral-gas density is high.

Discussion

We have shown that ion–neutral collisions enhance the thrust over power in the acceleration of plasma by electric and magnetic pressures. The simple 1D analysis provided certain scaling laws for the two accelerations. Enhanced thrust by electric pressure is being used in ionic wind acceleration schemes. The analysis here could be used to explore the use of magnetic pressure as well in the collisional regime for a high thrust scheme. The use of both magnetic field and applied voltage adds a flexibility relative to the use of electric pressure, for example by allowing the use of a relatively low voltage in a high thrust scheme.

In the analysis here we did not address the various sources of inefficiency and how they affect the efficiency of specific configurations. As in all thrusters, the issues of wall losses, ionization cost, and propellant utilization should be addressed. To model some of the issues associated with the collisions, kinetic models or simulations should be employed. We will address some of these issues in future experimental and theoretical research.

Acknowledgments The author thanks Gennady Makrinich for useful discussions. This research was supported by the Israel Science Foundation (Grant No. 765/11).

References

1. Goebel DM, Katz I (2008) Fundamentals of electric propulsion: ion and hall thrusters. Wiley, London
2. Makrinich G, Fruchtman A (2009) *Phys Plasmas* 16:043507
3. Makrinich G, Fruchtman A (2009) *Appl Phys Lett* 95:181504
4. Makrinich G, Fruchtman A (2013) *Phys Plasmas* 20:043509
5. Diamant K (2010) (Nashville : The 46 AIAA/ASME/SAE/ASEE Joint Propulsion Conference and Exhibit). AIAA 2010-6522
6. Hruby V, Pote B, Brogan T, Hohman K, Szabo J, Rostler P (2004) Air breathing electrically powered Hall effect thruster, Patent 6,834,492 USA
7. Burton KE (2000) Atmospheric fueled ion engine, Patent 6,145,298 USA
8. Go DB, Maturana RA, Fisher TS, Garimella SV (2008) *Int J Heat Mass Transf* 51:6047
9. Kim C, Hwang J (2012) *J Phys D Appl Phys* 45:465204
10. Gregory JW, Enloe CL, Font GI, McLaughlin TE (2007) (Reno: the 45th AIAA aerospace sciences meeting and exhibit). AIAA 2007-185
11. Sigmund RS (1982) *J Appl Phys* 53:891
12. Charles C (2009) *J Phys D Appl Phys* 42:163001
13. Fruchtman A (2011) *IEEE Trans Plasma Sci* 39:530
14. Greig A, Charles C, Hawkins R, Boswell R (2013) *Appl Phys Lett* 103:074101
15. Fruchtman A, Makrinich G, Ashkenazy J (2005) *Plasma Sour Sci Technol* 14:152
16. Fruchtman A (2008) *IEEE Trans Plasma Sci* 36:403
17. Godyak VA (1986) Soviet radio frequency discharge research. Delphic Associates, Falls Church
18. Lieberman MA, Lichtenberg AJ (2005) Principles of plasma discharges and materials processing, 2nd edn. Wiley, Hoboken
19. Raitses Y, Keidar M, Staack D, Fisch NJ (2002) *J Appl Phys* 92:4906
20. Gueroult R, Fruchtman A, Fisch NJ (2013) *Phys Plasmas* 20:073505